Acta Biomaterialia 159 (2023) 63–73

Contents lists available at ScienceDirect

Acta Biomaterialia

journal homepage: www.elsevier.com/locate/actbio

Full length article

Numerical model characterization of the sound transmission mechanism in the tympanic membrane from a high-speed digital holographic experiment in transient regime

J. Garcia-Manrique [a,b,c,*], Cosme Furlong [d,e], A. Gonzalez-Herrera [a], Jeffrey T. Cheng [b,c]

[a] Department of Civil Engineering, Materials and Manufacturing, School of Engineering, University of Malaga, Spain
[b] Eaton-Peabody Laboratory, Massachusetts Eye and Ear, Boston, MA, USA
[c] Department of Otolaryngology–Head and Neck Surgery, Harvard Medical School, Boston, MA, USA
[d] Center for Holographic Studies and Laser micro-mechaTronics (CHSLT), Worcester, MA, USA
[e] Mechanical Engineering Department, Worcester Polytechnic Institute, Worcester, MA, USA

ARTICLE INFO

Article history:
Received 27 July 2022
Revised 4 January 2023
Accepted 19 January 2023
Available online 26 January 2023

Keywords:
Finite element model
Acoustic–structural coupled analysis
Tympanic membrane
High-speed digital holographic
Sound transmission

ABSTRACT

A methodology for the development of a finite element numerical model of the tympanic membrane (TM) based on experiments carried out in the time domain on a cadaveric human temporal bone is presented. Using a high-speed digital holographic (HDH) system, acoustically-induced transient displacements of the TM surface are obtained. The procedure is capable to generate and validate the finite element model of the TM by numerical and experimental data correlation. Reverse engineering approach is used to identify key material parameters that define the mechanical response of the TM. Finally, modal numerical simulations of the specimen are performed. Results show the feasibility of the methodology to obtain an accurate model of a specific specimen and to help interpret its behaviour with additional numerical simulations.

Statement of significance

Improving knowledge of the dynamic behavior of the tympanic membrane is key to understanding the sound transmission system in human hearing and advance in the treatment of its pathologies. Recently we acquired a new tool to carry out experiments in transient regime by means of digital laser holography, capable of providing a large amount of information in a controlled transient test. In this work, these data are used to develop a methodology that generates a numerical model of the tympanic membrane based on numerical-experimental correlations. It is important to be able to develop models that fit specific patients. In this work, additional modal simulations are also presented that, in addition to validating the results, provide more information on the specimen.

1. Introduction

The study of the tympanic membrane (TM) has been a fundamental objective of the investigations concerning the mechanisms of sound transmission in the ear. The middle ear (ME) response to sound is affected by many interconnected parameters such as the complex geometries or the mechanical properties of various middle ear structures. Among them, the TM plays an important role to initiate the transmission of sound energy from the environment to the middle ear ossicular chain. Sound-induced motions of the TM show complex multiphasic patterns with frequencies [1–3], and in recent decades, both experimental and numerical approaches have been applied to study the mechanics of the TM for hearing.

Since the classical notion of the TM as a piston, numerous models have been developed to explain the mechanical response of the TM based on various experimental results on both humans and animals. Observations of frequency-dependent TM vibration modes from time-average holography (TAH) [1,2] and stroboscopic holography [3] suggest both standing waves and traveling waves on the TM surface, where traveling waves are consistent with the pres-

* Corresponding author.
E-mail address: josegmo@uma.es (J. Garcia-Manrique).

https://doi.org/10.1016/j.actbio.2023.01.048

ence of significant damping within the TM. Other observations of delays in the motions of the TM and the ossicles from the experiments carried out on cats lead to development of a transmission line model to help match the low impedance of the rim of the TM to the high impedance produced by the ossicular load at the TM's center [4]. On this basis, Goll and Dalhoff [5] developed their string model of the TM with distributed force. According to the dynamic response of a mechanical system, the TM surface motion is composed of the combination of different modal motions at different natural frequencies. These resonance frequency modes are summed at the manubrium attachment to the ossicular chain to produce a smooth transfer of sounds to the middle ear across all frequencies. Moreover, the phenomenon of reverse transmission from the tympanic cavity to the TM has also been studied and confirmed that a resultant standing-wave pressure field within the ME cavity [6,7].

Experiments have been and still are of great importance in these studies. Laser Doppler Vibrometry (LDV) is the most widely used technique to quantify the displacement of the TM at a single point (mostly at the umbo) at a time, in both magnitude and phase [8,9], and scanning LDV (SLDV) quantifies TM motions at a few hundred points across the entire TM surface [10]. Another technique developed in recent years is a fiber-optic-based optoelectronic holographic (OEH) interferometry system which can be operated in stroboscopic mode [11] to capture holographic images of the object which is illuminated by a train of brief laser pulses. Holographic methodologies have in fact been used in different studies to characterize TM parameters such as the TM contours [12], the three-dimensional shape and motion measurement in chinchillas [13], the characterization of acoustically-induced forces [14], the viscoelastic properties of the human TM [15] or recently, the correlation between TM displacement and TM thickness [16].

To develop a technique that is suitable for making measurements on live ears for clinical applications, a high-speed digital holographic (HDH) system has been developed [17]. HDH allows to measure TM movements produced by a short impulse (click) fast enough to ignore movement artifacts associated with physiological noise such as movements associated with breathing, heart beating, etc. The transient response captured by the high-speed camera (>50k frames per second) allows the analysis of TM impulse responses [18], in both normal and experimentally simulated pathological human middle ears [19]. Recently, Tang et al., [20] used the HDH to record human cadaveric TM transient responses induced by acoustic impulses. They developed frequency and impulse analyses to identify several new TM mechanical parameters including (i) dominant frequencies, (ii) rising time, (iii) exponential decay time over the complete TM surface. It was also study the frequency dependent damping of the middle ear system based on the TM full-field frequency and impulse responses. These studies show a high potential of this experimental technique to gain insight into TM mechanics. However, there are also challenges to understand and interpret a large dataset like this, i.e. TM surface motions with high spatial and temporal resolutions over 100,000 points on the TM surface per image frame and ~ 80,000 frames per second over ~10 milliseconds, which yields a ~100 MByte dataset per measurement.

In addition to experimental measurements, numerical simulations are proving to be a necessary tool to help interpret experimental results or guide the experiment. Since the first works on numerical models on cats' eardrums [21,22] or on the behavior of the middle ear in humans [23,24], finite element models (FEMs) of the auditory system have evolved considerably [25–28] The three-dimensional finite element models of the auditory system make it possible to represent complex geometry of the ear more accurately [25,26,28–30]. Great efforts have been made to determine realistic material properties of middle ear structures represented in the model [29,31–35]. Other approach is to focus on main physical phenomena implied in the process using simplified models. In these works, systems equivalent to specific parts of the hearing transmission mechanism are modeled using simple models. This allows different mechanisms to be separated and studied, such as the tube-membrane system, which helps to better understand the coupling of the ear canal and the eardrum, or the predeformation in the TM, which helps to understand its influence on the main frequencies [36,37].

The majority of prior finite element models of the ear are based on steady-state responses of the ear to harmonic excitations or directly on the modal analysis of the middle ear system. However, due to the complexity and the computational cost of the simulation of time-domain responses of the human auditory system, there are only a few work in literature. Zhang et al. [27] presented a finite element model to simulate transient responses of the human ear to two idealized short-duration impulses. It is an interesting model because it is one of the few works in the literature that has managed to simulate the human auditory system in the time domain. However, their model simulations have not been experimentally verified.

This paper presents a novel methodology to develop a FEM of a specific human middle ear specimen by comparing time domain numerical simulations of the TM transient responses induced by acoustic clicks with the HDH test results [20]. The material parameters of the FE model were adjusted to fit the dynamic behaviors of the TM from the model to the experiment. The ultimate goal is to develop a realistic finite element model of the human auditory system that can be used to enhance our understanding of the working mechanisms of the ear and assist in diagnoses of middle ear pathologies. This paper presents the preliminary results of this methodology.

We present our methodology in two parts. Part 1 will briefly describe our HDH experiments conducted on cadaveric human ear specimen and data analyses (details can be found in [20]); and part 2 describes the creation of the numerical FE model and the tuning of material parameters to fit the modeling results with the experimental datasets. Based on the final tuned model in transient regime, a modal analysis of the system is performed to help interpret the experimental data. Finally, the main conclusions of the paper will be discussed.

2. Experiments and data analyses

2.1. High-speed digital holographic tests of human tympanic membrane

This section contains a brief review of our HDH experimental measurements of the TM transient vibrations induced by acoustic clicks. The fundamentals and details of displacement measurements by holography can be found in our papers [20,38–40]. Our HDH system is capable of measuring the shape and the displacement at more than 100,000 points per TM surface, with a temporal resolution < 20 μs and a displacement resolution ~10 nm. The lateral resolution for the shape measurement is around 100 μm. Therefore, a rich dataset containing both the full-field displacement of the TM and the shape (taper) of the TM.

A fresh human post-mortem temporal bone from which the cartilaginous and bony ear canal parts were removed was used for the experiment. The normality of the middle ear was visually checked by means of facial recess opening. Once checked, the opening was sealed with sealing cement to ensure a closed middle ear cavity. The specimen was placed in the HDH system as shown in the Fig. 1 and the outer surface of the TM was painted with a thin layer of white paint to increase laser reflectivity, which does not affect TM motions as shown in our prior studies [2,3,20]. The system has two lasers coupled in the same optical path, a 532 nm

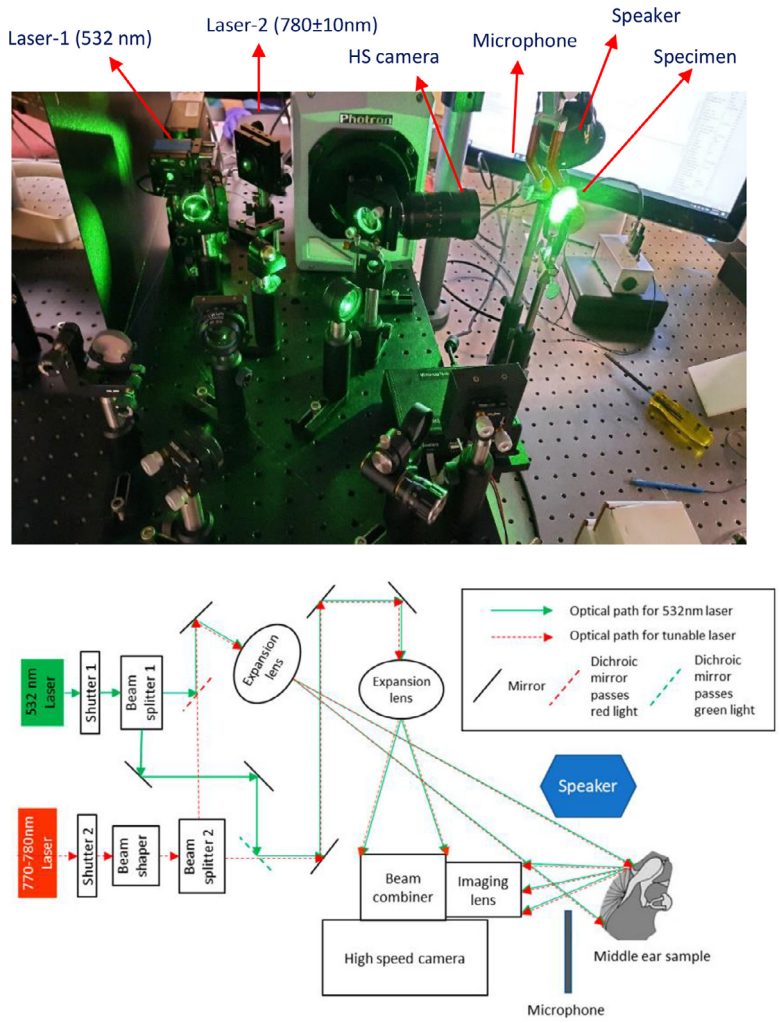

Fig. 1. Experimental setup and Scheme of the HDH system [19].

laser to measure the displacement and a tunable 770-780 nm laser to measure the shape. The experiment consisted in measuring the transient response of the TM to a short acoustic click generated by the speaker (50μs square wave). In addition to the measurements obtained from the TM, measurements from a microphone (Knowles FG-23329) within a few mm from the TM annulus are also recorded to monitor the stimulus profile near the TM surface, which will be used as input to FE model.

Displacement measurements were based on correlation interferometry capable of measuring the full-field displacements of the visible lateral TM surface (>100,000 points at 67,200 fps camera frame rate) by applying Pearson's correlation [17,38,40]. The shape measurement is based on the Multiple Wavelength Holographic Interferometry (MWHI) by means of variations in the wavelength of illumination with a constant optical path length (OPL) [38,41–43].

2.2. Experimental results

Fig. 2 shows the acoustic waveform recorded by the microphone from one of the holographic displacement measurements. The microphone measurement is phase locked to the triggering signal sent to the speaker to generate the acoustic click, and there is about 3.65 ms delay between the electrical triggering signal and the acoustic wave arriving the microphone. The microphone continuously samples the signal every 2 μs for 25 ms. As shown in Fig. 2, the acoustic waveform shows a click like signal and the

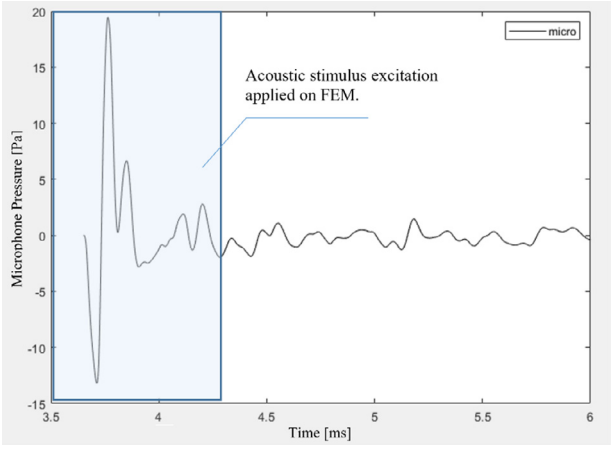

Fig. 2. Acoustic waveforms recorded by Microphone from one of the holographic measurements.

magnitude of the waveform dampens out quickly after just a few ms. Noted between the speaker and the microphone there are optical parts of the system which can introduce bounced acoustic signals that will be sensed by the microphone. Nevertheless, the acoustic signals recorded by the microphone included the real time acoustic stimulus that excites the vibration of the TM and

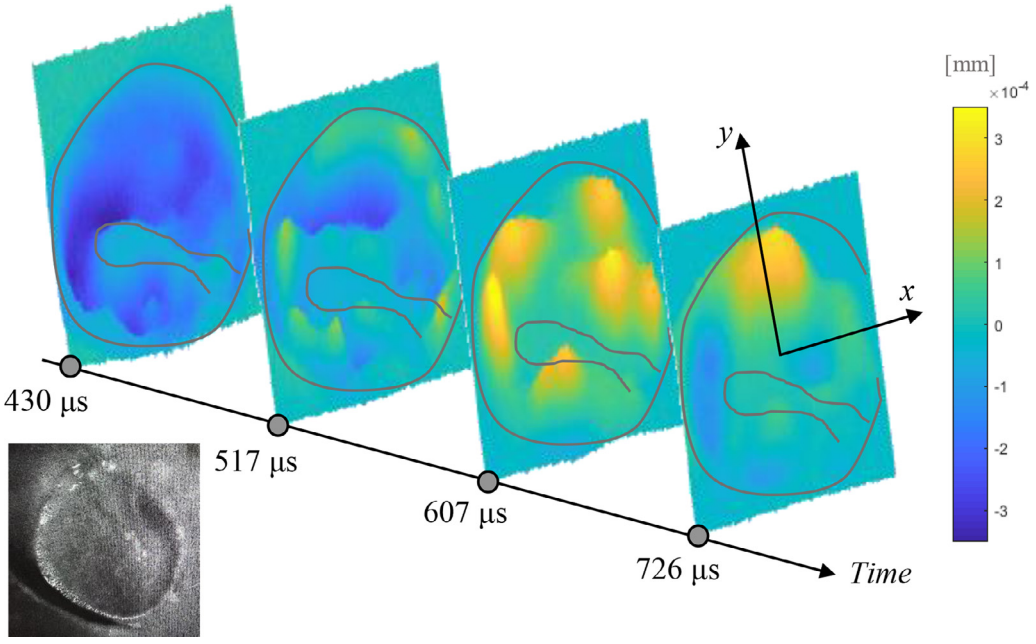

Fig. 3. Normal Surface Displacement data from one specimen (TB-3) during different moments in HDH experiment.

bounced acoustic signals reflected from surroundings. The recording obtained in the first phase of the experiment (shaded area in Fig. 2) is introduced as a source of excitation in the numerical model, given the signals after that time may capture reflected signals and it is difficult to separate them out.

The displacements of the TM over the same period of time are also available at the same data collection frequency (67.200 Hz). The data are collected on a 512×512 mesh equi-spaced across the surface. While processing of the information collected, smoothing techniques are applied so that each point represents average of an interval of adjacent points [20].

By applying the MWHI technique, the shape of the outer wall of the membrane is also available. The information on the shape, together with the observer's positions, also allows to determine the surface normal vectors and the direction of displacement [38]. Fig. 3 shows the results from different moments of the experiment corresponding to the normal displacements to the TM surface in one of the specimens (complete datasets can be found in [20]).

3. Numerical modeling methodology – finite element model

3.1. Assumptions of the model

The main objective is to obtain a finite element model that can be used to simulate and characterize the dynamic response of a human TM based on dataset from the holographic test of a specific human specimen. Many finite element modeling work of the middle ear including the TM have been reported in the literature, however, few has been performed in time domain, which is computationally more demanding than simulations in frequency domain or harmonic analysis, and difficult to validate experimentally. To facilitate simulation of the TM transient response in time with finite element modeling, we applied several assumptions and simplifications of our modeling approach below:

- Our model will not have middle ear components, such as three middle ear ossicular bones, at the current stage. The effect of the ossicular chain on the TM is simulated by coupling a series of mass and spring elements to the umbo area of the TM and acting on the properties of TM in contact with malleus.
- We identify the damping characteristics of the TM based on the experimental datasets and applied two damping values to the TM model, one along the manubrium region of the TM (to account for impedance loading from the middle ear) and the other for the rest of the TM area.
- We consider homogeneous and constant value of the Young's modulus of the TM based on the assumption that the deformation of the TM under the test is not high enough to trigger its nonlinear working section of the stress-strain curve. The peak sound pressure of acoustic click is less than 20 Pa or 120 dB SPL (Fig. 2), which does not induce nonlinear vibration of the middle ear [44].
- We further assume a constant TM thickness in our TM model. Although there are studies showing the TM thickness varies with location, we do not consider the thickness effect in the current model.

Based on these assumptions and simplifications, a working methodology has been developed accordingly. The geometry of the TM model was created based on the experimentally measured TM shape contour and then extended to a 3-dimensional model with a uniform thickness. The model parameters are adjusted by numerical-experimental validation between the test and a series of numerical simulations in transient regime. These parameters include: the equivalent mass and stiffness of the ossicular chain (added to the umbo area), the mass and the stiffness characteristics of the TM (Young's modulus (E) and thickness (th)) and two damping values; one related to TM and the other related to middle ear component effects. To reduce the number of iterations the analysis focuses on the stiffness property, considering a given constant thickness throughout the membrane.

3.2. Geometry and mesh

The shape of the TM obtained from MWHI measurement is loaded into a CAD reconstruction software to model the conical shape of the TM with a mesh of 512×512 geometric points (Fig. 4a). A subroutine identifies the contours of the malleus (moving differently from the rest of the TM) and the TM anulus (fixed boundary without motion) and creates a logical mask to fix the

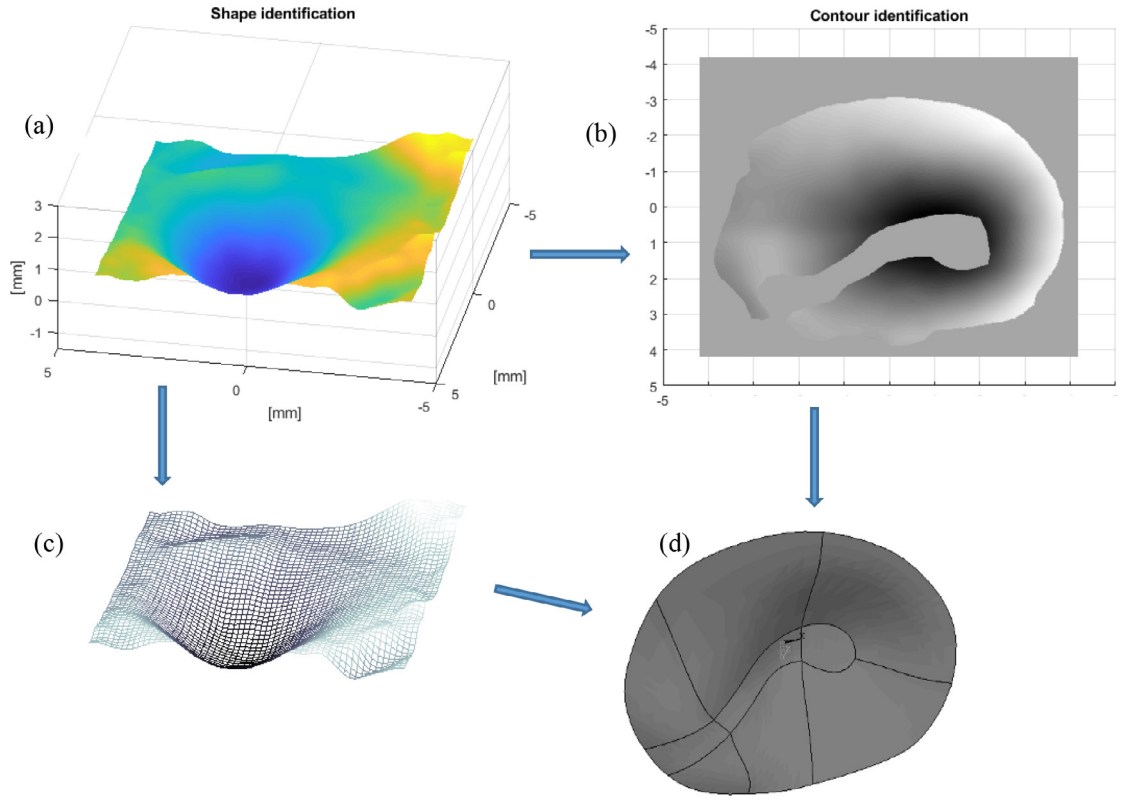

Fig. 4. Automatic generation of the model geometry, boundary condition and mesh. (a) Surface obtained from MWHI. (b) Logical Mask of boundary identification applied to TM. (c) point cloud data to export to FEM software. (d) Areas that define the TM surface shape of the specimen in ANSYS.

boundaries of TM (Fig. 4b). Combining an equi-spacing cloud of points (Fig. 4c) obtained from the geometry and the logical mask, a set of areas is generated in FEM software that corresponds to the TM of the specimen (Fig. 4d). TM annulus is fixed with zero displacement in all three axial coordinates as a boundary condition.

The simulations were carried out with ANSYS software (ANSYS Academic Multiphysics Campus Solution Research, version 2020-R2). Pre-processing and Post-processing data is carried out with MATLAB software (version 2018 and 2020).

The volume is then defined given the assumption of constant thickness. The routine generate point-to-point offset tools that can be used to generate variable thicknesses for future calculations. To simulate acoustic and structure interference air volumes are generated on both sides of the TM volume (Fig. 5b) to represent the ear canal and middle ear air spaces. The ear canal side air volume shall be large enough to cover simulations of sound transmissions at multiple frequencies in the range of audible sound frequencies that goes from 50 Hz to 20 kHz. The dimensions of the middle ear cavity side volume are similar to the reported middle ear cavity volume. In both cases a transition volume is generated between the TM and the air volume to allow the simulation of the fluid-structure coupling in the calculation (Fig. 5a)

The mesh strategy is similar to previous works [36,37,45]. TM structure presents a regular mesh with cubic elements with 8-nodes (SOLID185 in ANSYS) and a maximum element size of three times the membrane thickness. Air volumes are meshed with FLUID30 with pressure activated as the degree of freedom, except that at the interface region where both pressure and displacement are activated as the degrees of freedom. Element FLUID130 provides the ability to simulate far field acoustic and are introduced in the outer surface of external air volume. In baffle areas around TM and contour of inner air volume, closed cavity boundary conditions are applied and there exist full reflection in those surfaces. Element size is limited by the tenth part of the minimum wavelength considered (frequency of 20 kHz). There is a controlled transition from external element size in air (1.17 mm) to air element in contact with TM (150 µm). This model also introduces spring-type and mass-type elements uniformly connected normal to the surface on the 100 nodes of the umbo region to simulate loading from the ossicular chain (without any actual middle ear structures).

The excitation surface is defined as an area inside the outer volume air with an inclination of 45º and 10mm from the center of the TM. The excitation is applied as a uniform pressure in time step of the simulation. In the following sections, we will discuss how to determine the damping, mass and stiffness of the model.

3.3. Damping

Several different approaches have been applied to characterize damping in the human auditory system. Among them, the most common is to apply the Rayleigh model (αM+ βK) with different values to all the elements of the middle ear system: α=0 s^{-1} and β=7.5×10^{-5} s [25,27], α=0 s^{-1} and β=10×10^{-5} s [28,30] or α=260 s^{-1} and β=3.7×10^{-5} s [46]. Other models apply viscoelastic behavior defined through a loss factor η (Ω) relating the elastic Young's modulus and the viscous parameter with different values of η such as in [47] (of 1% at 20Hz up to 13% at 20 kHz) or in [48] (constant 7.8% at all frequencies). In 2014, De Greef et al. [15] compared both options with stroboscopic holography and FEM, concluding that constant or moderately increasing loss factor provided a better correlation than Rayleigh model at higher frequencies.

While all these values gave good approximations in the 1 kHz range, the viscoelastic models performed better at higher frequencies. Damping is, as can be seen from the great variability of results, one of the most complex parameters to describe and specify in any dynamic system. Different strategies to approximate the

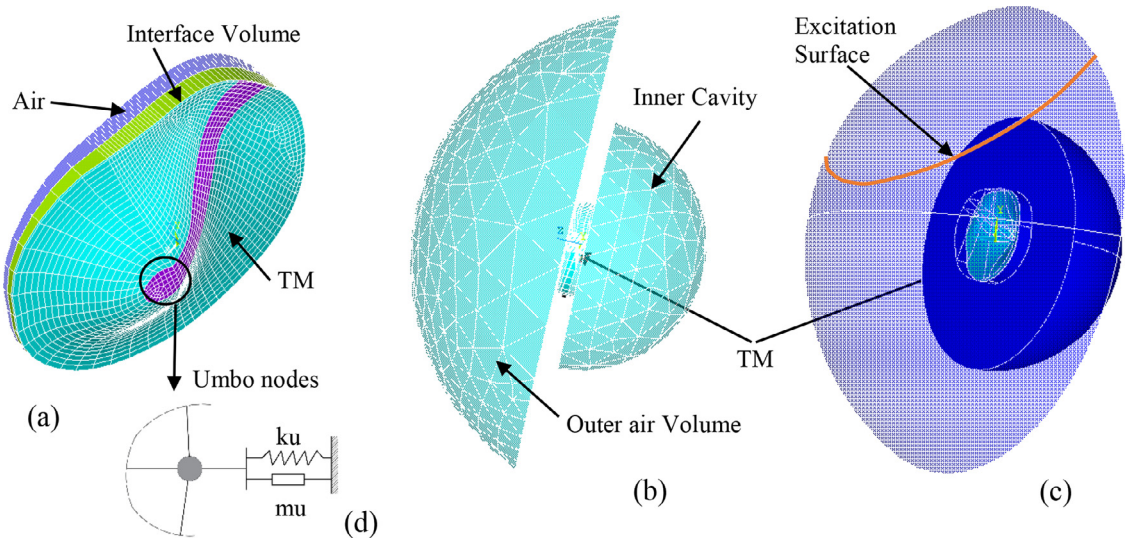

Fig. 5. Finite Element Model. (a) TM meshed volume and fluid-structure interface (b) air regions around TM (c) Position of stimulus in outer air volume (d) parameter model of mass-element (mu) and spring-element (ku) connected to each node of umbo region.

damping can be established directly from the time-domain experimental results. The damping of this specific TM specimen has already been analyzed in Tang et al. [20] (from TB3), which suggests an average damping ratio (ratio of actual damping to critical damping) of 0.4 with dominant frequencies near 1 kHz and 0.1 to 0.2 with dominant frequencies around 2.5 kHz (Fig. 18 in [20]).

In this case, for the transient numerical simulation, two different damping values have been applied. Two damping ratios are introduced in the model, $\xi 1$ is applied to the general volume of the TM, and $\xi 2$ is applied to the manubrium region of the TM in contact with the malleus. Together with the additional umbo elements described above, $\xi 2$ allows to characterize the effect of the response of the internal cavity elements on the TM. It introduces an additional damping to umbo region. This zone tends to have larger damping than the rest of the TM [20].

A methodology similar to the previous one has been applied but isolating the most representative areas for $\xi 1$ and $\xi 2$. To this end, an intermediate membrane zone between the anulus and the malleus has been isolated where the cross-membrane effects with these regions can be minimized. Using an approximation exponential to the results of the displacements over time, the parameters of each node have been adjusted. A filter was previously applied to eliminate the initial response in order to study the system without external disturbances. $\xi 2$ is obtained with the same methodology applied to a selection of nodes in the central axis of the malleus. The average of the calculated adjustments of all the nodes in these areas are $\xi 1 = 3.5\%$ and $\xi 2 = 6\%$.

3.4. Material characterization

Material properties used in our numerical FE model of human TM are listed in Table 1. In addition to damping discussed above, the air element characteristics and a constant Poisson ratio of 0.3 are adapted from the literature. The most uncertain parameter is the Young's modulus (E) of the TM. The literature presents a range of very disparate E values, from 3MPa [48], to the more general range of 20-40 MPa with either homogeneous value [30,34] or different values between radial and circumferential directions [25]. In 2005, Fay et al. [49], argued that these values were underestimated and proposed a range between 100 and 300 MPa. The range we chose in this study to iterate the numerical-experimental fit is therefore very wide.

Table 1
Material properties used for eardrum FE numerical simulations.

Component	range of variables	FEM solution
Tympanic membrane		
Thickness (μm)	50	50
Density d1 (kg/m^3)	1200-1800	1500
Young Modulus E1 (MPa)	20-40	32
Damping (%)	3.5	3.5
Volume of Tympanic membrane in contact with malleus (Equivalent system for ossicular chain)		
Thickness (μm)	50	50
Density d2 (kg/m^3)	10^4 - 10^5	7×10^4
Young Modulus E2 (MPa)	10^5 - 10^6	8×10^5
Damping (%)	6	6
Additional Elements in umbo region (Equivalent system for ossicular chain)		
Spring Constant Ku	0-10	2
Mass elements mu (kg)	10^{-9} – 10^{-7}	2×10^{-7}
Air		
Density (kg/m^3)	1.21	1.21
Sound speed (m/s)	343	343

In the present study, a constant TM thickness of 50 μm has also been set in line with previous work. Two values of TM stiffness (th-E binomial) are used, one for the membrane (E1) and other for the malleus region (E2). In addition, the values of the density of the same regions (d1 and d2) and the stiffness (ku) of the springs and the mass (mu) of the mass-type elements attached to the umbo are also adjusted.

The stimulus is applied in the excitation surface (see Fig. 5c) during first 0.5ms of the simulation (see Fig. 2). The simulation in transient regime is carried out with the same time step as the real experiment. In the same way, the input signal is introduced with the same data and at the same intervals as the one recorded by the microphone.

A campaign of numerical simulations has been programmed and carried out to adjust these values (E1,d1,E2,d2,ku,mu). More than 400 simulations have been carried out. A correlation of the time domain displacement response of a number of selected points in different areas of the TM (Fig. 6) was carried out between transient numerical simulations and test datasets. The nodes have been selected due to their representativeness in the movements observed in each area studied.

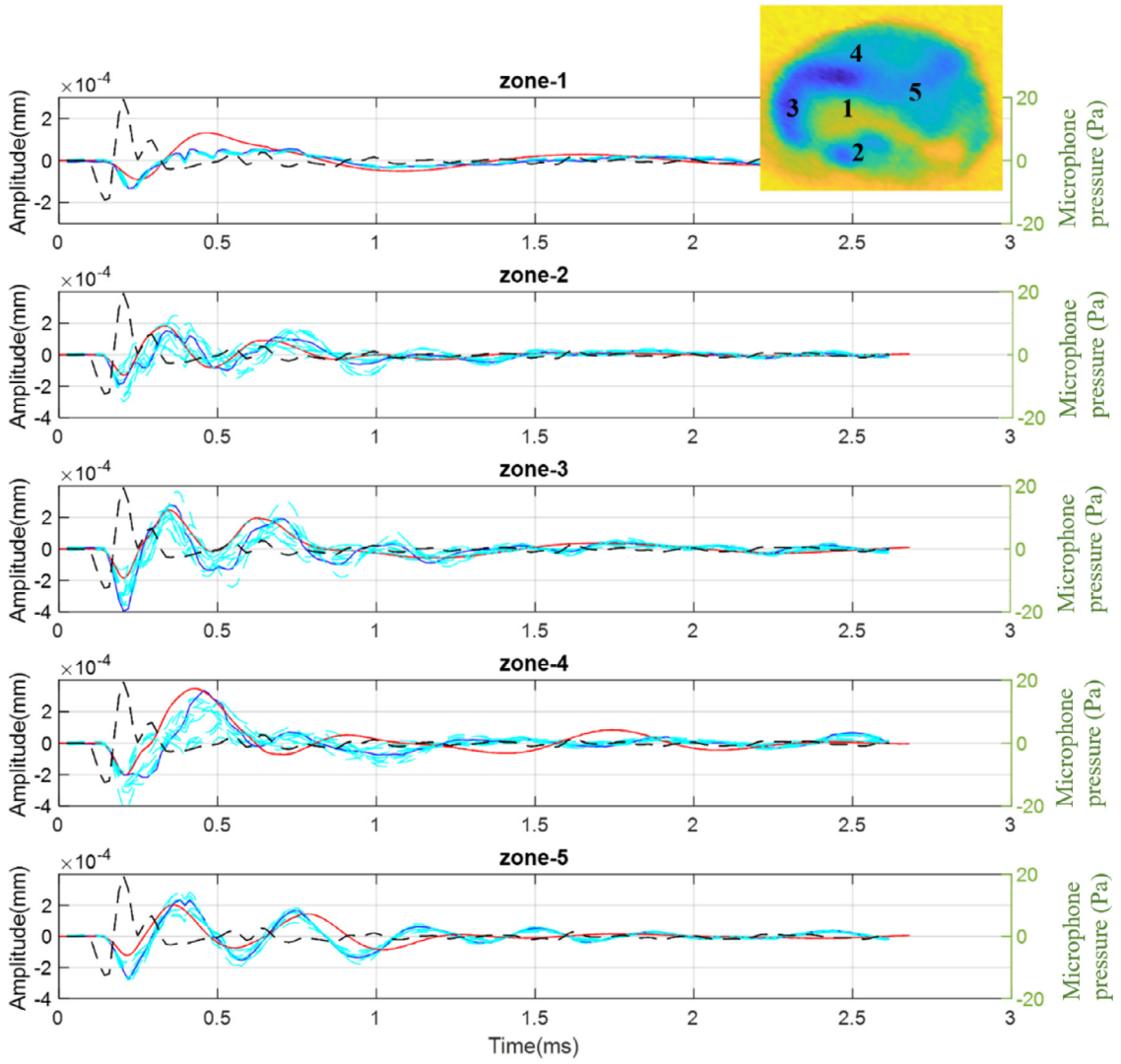

Fig. 6. Transient evolution of normal displacement of the TM from experimental results (cyan lines) and numerical simulation (red lines). Dash lines show the micro signals records. (For interpretation of the references to colour in this figure legend, the reader is referred to the web version of this article.)

The iterative method used to change parameter was divided in four steps:

- Keep all the parameters in Table 1 at their median values except the Young's modulus E2 and density d2 of the malleus region. Iterate E2 and d2 values until the model predicted displacements at the umbo region of the TM agree with those obtained in the experiment.
- With the above, iterate values of E1 and d1 of the tympanic membrane until displacements of selected nodes (zones 2, 3, 4 and 5) from the model agree with those obtained in the experiment.
- With the above, iterate values of Ku and mu of the equivalent system of the ossicular chain until the model derived dominant frequencies, successions of maximums and minimums at umbo region on a time scale, are similar to those from the experiment.
- Fine adjustment from previous values to optimize modelling results.

Fig. 6 compares the FEM simulations of the TM motions with experimental results at five locations of the TM as marked in an inserted TM surface motion map. Zone-1 is at the umbo of the TM, and Zones 2 to 5 are four locations arranged around the manubrium. In Fig. 6 dash lines represent microphone recorded sound pressure signals, cyan lines represent experimental results (from multiple locations within each region) and red lines represent the FEM solution from a single point within each region on the TM surface. The figure compares transient displacements of the TM from different regions within the first 2.7 ms between the experiment and modeling. The numerical model replicates relatively well the displacement patterns and displacement amplitudes of the TM motion of the experiment. The first peak of the displacement in Zones 1 and 4, and the first and second peaks of the displacement in Zones 2, 3 and 5 are all captured in numerical simulations.

Fig. 7 present selected frames from both experimental (Fig. 7a) and numerical (Fig. 7b) results in the range of 0.2-0.46 ms. Similar TM surface motion patterns, i.e. displacement peaks (in yellow) and valleys (in blue) circumferentially arranged around the manubrium of the TM, between the experiment and modeling are observed at the same time instant throughout the selected time course. This similarity suggests the objective of reproducing the experimental behavior of the TM in our FE TM model has been achieved.

The main dynamic data deduced from correlations give us the following average values for the tympanic membrane: E1=32 MPa;

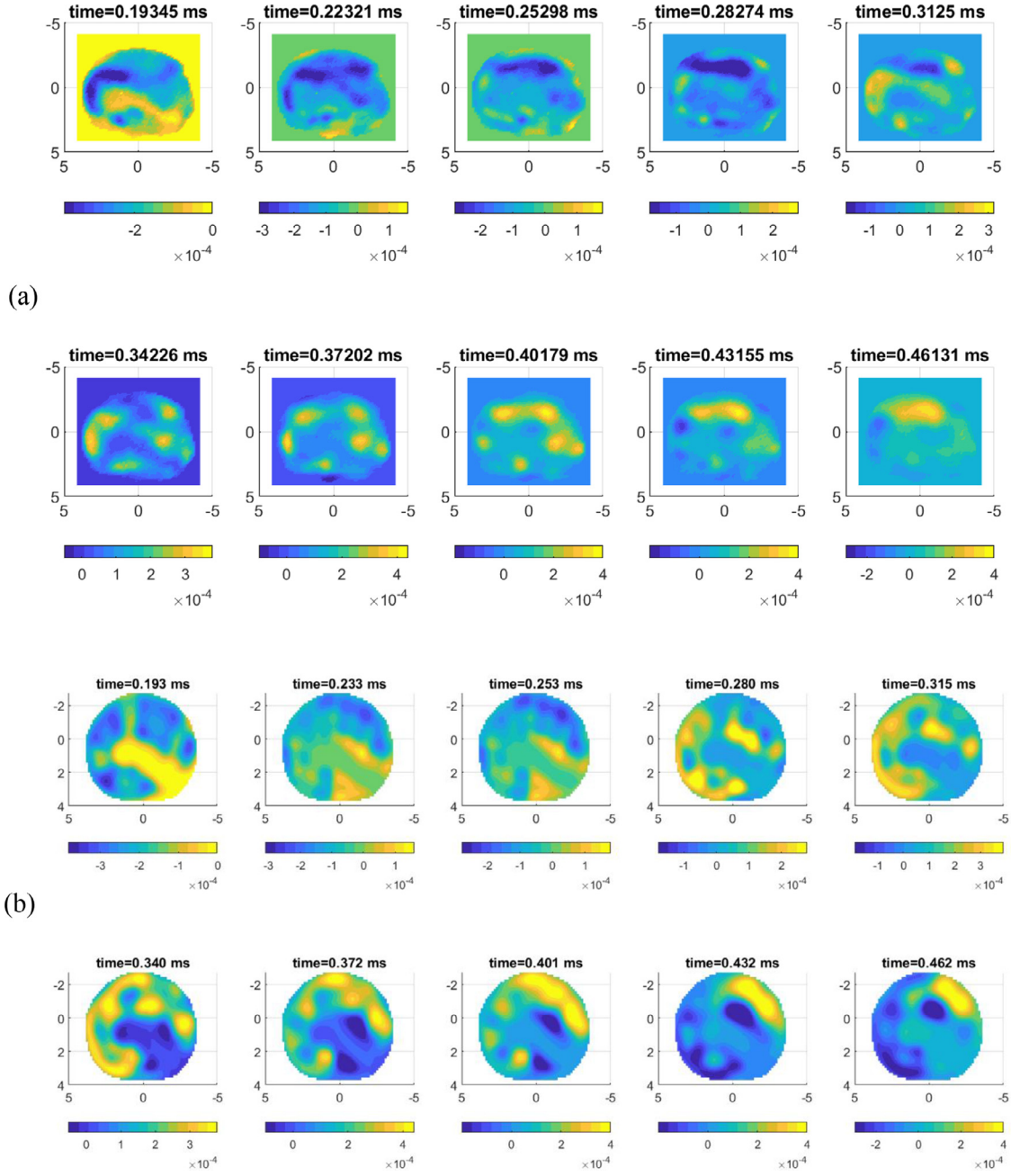

Fig. 7. Results from selected frames in 0.2-0.46ms time range. (a) surface displacement from test specimen. (b) surface displacement from numerical model.

d1= 1500 Kg/m^3; E2=8×10^5 MPa; d2= 70000 Kg/m^3 . With them, the model is defined and can be used in further simulations to complement the analysis of the experimental datasets.

4. Application of FEM to identify modal shapes of the TM response

In this section we introduce results from a modal analysis using our developed FEM of the TM to complement the TM results obtained exclusively through the tests [20]. In that paper the dominant frequencies of the TM were obtained based on Frequency Response Function (FRF) at each point of the TM surface, but they are limited to a limited number of identified dominant frequencies because the identification algorithm is based on average values of five zones of the TM. However, some studies [28,50] have suggested the TM may have much more closely spaced (in frequency domain) resonance frequencies (or dominant frequencies). A modal simulation is the right tool to further understand the resonance frequencies of the TM involved.

Fig. 8 presents the results of the modal simulation applied to the finite element TM model developed in this study. Much more natural frequencies from the TM model are identified as well as their associated mode shapes. The model may not account for the resonance frequencies associated with the vibration modes of the ossicular chain due to simplification of the middle ear [28]. Each image in Fig. 8 represents a mode shape of TM vibration with mode number (M) and the associated natural frequency. Due to significant changes of the absolute values of the TM displacement with frequency, all the images are scaled between maximum and minimum value of the displacement on the TM surface at each in-

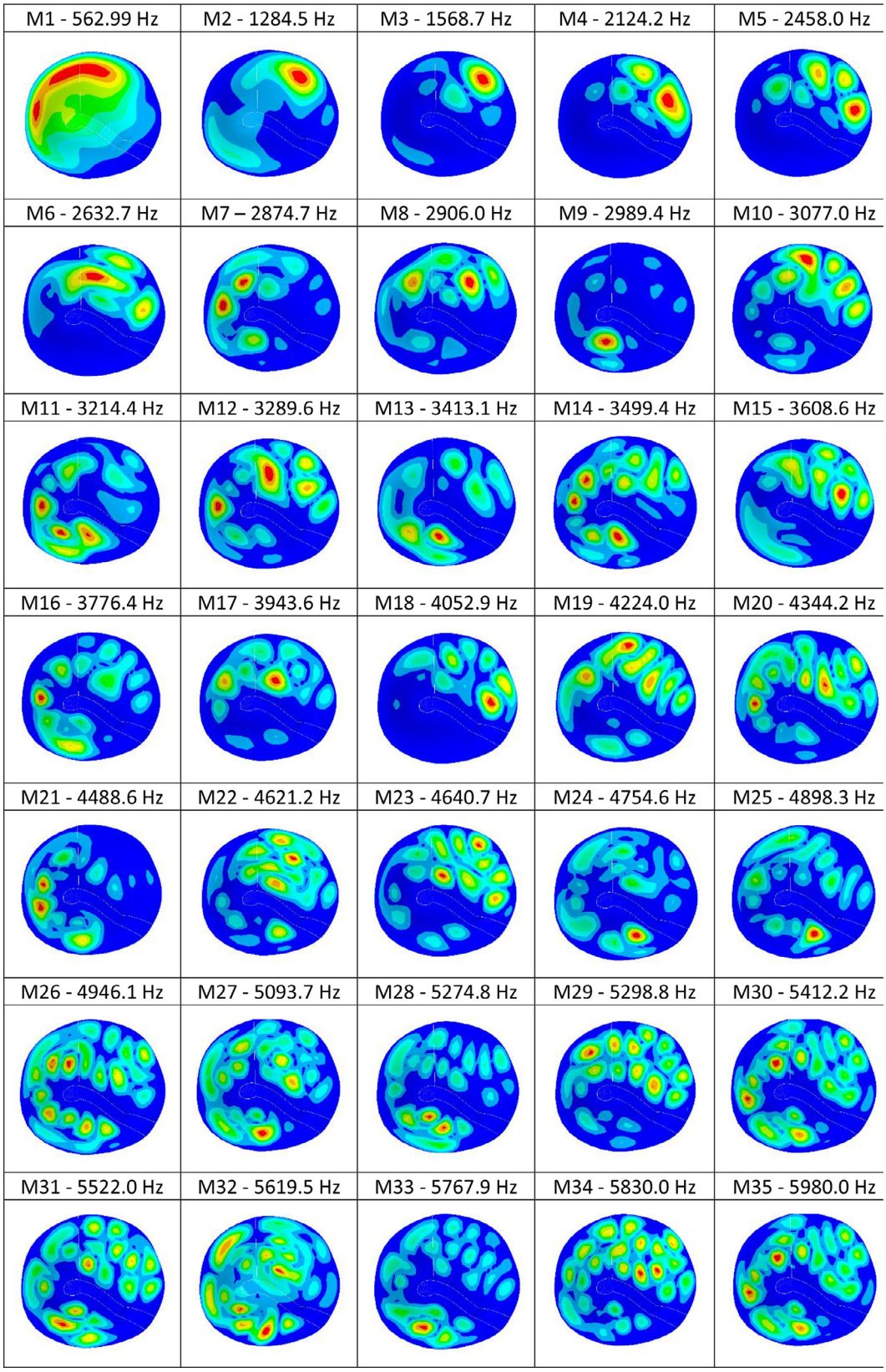

Fig. 8. Natural frequencies and modes shapes from modal simulation of the specimen.

dividual mode, where the red color represents the maximum displacement on the TM surface, and blue represents the minimum displacement of the TM.

The resonance frequencies of the TM around 1.2 kHz (M2) and 1.5 kHz (M3) obtained here are consistent with the experimental results from the same specimen (TB3) presented in [20], where dominant frequencies between 1 and 1.5 kHz at five regions of the TM were identified (see Fig. 11(b) in [20]). However, our modal simulation allows us to expand and identified much more resonance frequencies. In [20] if we focus on the map of dominant frequency results for TB3 (Fig. 11(a) in [20]), it can be observed a few regions around manubrium with dominant frequencies of 2000-2800 Hz (in orange color), which are consistent with Fig. 8 (modes M3 to M8).

5. Conclusion

HDH is shown as a tool with great potential. The huge number of points and information related to them allows to obtain a complete geometry of the membrane surface and export it with good results to CAD tools. The differences detected in time-domain behavior also allow identifying and automating the separation of zones with different behavior such as the malleus or the annulus. Again, it allows to automate the generation of boundary conditions in a numerical model.

In this work, it has been demonstrated a methodology that allows simulating in a transitory regime a numerical model that recreates the holography test carried out in the laboratory. It has been possible to mechanically characterize the target dynamic parameters by performing a huge number of numerical simulations and, by means of an iterative protocol of experimental and numerical correlations, results with good similarity have been obtained.

We attempted using the model as a tool to complement the results obtained experimentally. Specifically, modal analysis results of the specimen are presented, which expanded identifications of the dominant frequencies in the system.

In future work, more quantitative analyses will be developed to better assess similarity between experimental results and numerical results. Likewise, this methodology will be extended to more specimens that have already been tested. Differentiation between healthy specimens and specimens with induced middle ear pathologies are currently being carried out to test the clinical diagnostic value of the model.

On the other hand, it is necessary to advance in the optimization of the iterative process to fit modeling simulation with experimental dataset and reduce the computation time. This numerical model can also be expanded by introducing additional elements of the middle ear, such as the ossicular chain.

Declaration of Competing Interest

The authors declare that they have no known competing financial interests or personal relationships that could have appeared to influence the work reported in this paper.

Funding

This work has been funded by the University of Malaga/CBUA, the FEDER program grant number UMA18-FEDERJA-214 and by the National Institutes of Health (NIH), National Institute on Deafness and Other Communication Disorders (NIDCD), grant number R01, DC016079. This research has also been partially supported by Research Grant Jose Castillejo number CAS19/00125 from Spain Government.

References

[1] S.M. Khanna, J. Tonndorf, Tympanic membrane vibrations in cats studied by time-averaged holography, J. Acoust. Soc. Am. 51 (1972) 1904–1920, doi:10.1121/1.1913050.
[2] J.J. Rosowski, J.T. Cheng, M.E. Ravicz, N. Hulli, M. Hernandez-Montes, E. Harrington, C. Furlong, Computer-assisted time-averaged holograms of the motion of the surface of the mammalian tympanic membrane with sound stimuli of 0.4-25 kHz, Hear. Res. 253 (2009) 83–96, doi:10.1016/j.heares.2009.03.010.
[3] J.T.J.T. Cheng, M. Hamade, S.N.S.N. Merchant, J.J.J. Rosowski, E. Harrington, C. Furlong, Wave motion on the surface of the human tympanic membrane: holographic measurement and modeling analysis, J. Acoust. Soc. Am. 133 (2013) 918–937, doi:10.1121/1.4773263.
[4] S. Puria, J.B. Allen, Measurements and model of the cat middle ear: evidence of tympanic membrane acoustic delay, J. Acoust. Soc. Am. 104 (1998) 3463–3481, doi:10.1121/1.423930.
[5] E. Goll, E. Dalhoff, Modeling the eardrum as a string with distributed force, J. Acoust. Soc. Am. (2011), doi:10.1121/1.3613934.
[6] R.D. Rabbitt, A hierarchy of examples illustrating the acoustic coupling of the eardrum, J. Acoust. Soc. Am. 87 (1990), doi:10.1121/1.399050.
[7] C. Bergevin, E.S. Olson, External and middle ear sound pressure distribution and acoustic coupling to the tympanic membrane, J. Acoust. Soc. Am. 135 (2014) 1294–1312, doi:10.1121/1.4864475.
[8] R.Z. Gan, M.W. Wood, K.J. Dormer, Human middle ear transfer function measured by double laser interferometry system, Otol. Neurotol. 25 (2004) 423–435, doi:10.1097/00129492-200407000-00005.
[9] J.J. Rosowski, H.H. Nakajima, S.N. Merchant, Clinical utility of laser-Doppler vibrometer measurements in live normal and pathologic human ears, Ear Hear. (2008), doi:10.1097/AUD.0b013e31815d63a5.
[10] O. de La Rochefoucauld, E.S. Olson, A sum of simple and complex motions on the eardrum and manubrium in gerbil, Hear. Res. 263 (2010) 9–15, doi:10.1016/j.heares.2009.10.014.
[11] J.T.J.T. Cheng, A.A.A.A. Aarnisalo, E. Harrington, M.D.S.M. del S. Hernandez-Montes, C. Furlong, S.N.S.N. Merchant, J.J.J. Rosowski, Motion of the surface of the human tympanic membrane measured with stroboscopic holography, Hear. Res. 263 (2010) 66–77, doi:10.1016/j.heares.2009.12.024.
[12] S.M. Solís, M. del S. Hernández-Montes, F.M. Santoyo, Tympanic membrane contour measurement with two source positions in digital holographic interferometry, Biomed. Opt. Express. 3 (2012) 3203, doi:10.1364/BOE.3.003203.
[13] J.J. Rosowski, I. Dobrev, M. Khaleghi, W. Lu, J.T. Cheng, E. Harrington, C. Furlong, Measurements of three-dimensional shape and sound-induced motion of the chinchilla tympanic membrane, Hear. Res. 301 (2013) 44–52, doi:10.1016/j.heares.2012.11.022.
[14] M. Khaleghi, C. Furlong, J.T. Cheng, J.J. Rosowski, Characterization of acoustically-induced forces of the human eardrum, in: Conf. Proc. Soc. Exp. Mech. Ser., 2016, doi:10.1007/978-3-319-21455-9_18.
[15] D. De Greef, J. Aernouts, J. Aerts, J.T. Cheng, R. Horwitz, J.J. Rosowski, J.J.J. Dirckx, Viscoelastic properties of the human tympanic membrane studied with stroboscopic holography and finite element modeling, Hear. Res. 312 (2014) 69–80, doi:10.1016/j.heares.2014.03.002.
[16] C.V. Santiago-Lona, M. del S. Hernández-Montes, M.F. Moreno, V. Piazza, M. de la Torre, C. Pérez-López, F. Mendoza-Santoyo, A. Sierra, J. Esquivel, Tympanic membrane displacement and thickness data correlation using digital holographic interferometry and confocal laser scanning microscopy, Opt. Eng. (2019), doi:10.1117/1.oe.58.8.084106.
[17] P. Razavi, J.T. Cheng, C. Furlong, J.J. Rosowski, High-speed holography for in-vivo measurement of acoustically induced motions of mammalian tympanic membrane, in: Conf. Proc. Soc. Exp. Mech. Ser., Springer, New York LLC, 2017, pp. 75–81, doi:10.1007/978-3-319-41351-8_11.
[18] P. Razavi, H. Tang, J.J. Rosowski, C. Furlong, J.T. Cheng, Combined high-speed holographic shape and full-field displacement measurements of tympanic membrane, J. Biomed. Opt. 24 (2019), doi:10.1117/1.JBO.24.3.031008.
[19] H. Tang, P. Razavi, K. Pooladvand, P. Psota, N. Maftoon, J.J. Rosowski, C. Furlong, J.T. Cheng, High-speed holographic shape and full-field displacement measurements of the tympanic membrane in normal and experimentally simulated pathological ears, Appl. Sci. (2019), doi:10.3390/app9142809.
[20] H. Tang, P. Psota, J.J. Rosowski, C. Furlong, J.T. Cheng, Analyses of the tympanic membrane impulse response measured with high-speed holography, Hear. Res. 410 (2021), doi:10.1016/j.heares.2021.108335.
[21] W.R. Funnell, C.A. Laszlo, Modeling of the cat eardrum as a thin shell using the finite-element method, J. Acoust. Soc. Am. 63 (1978) 1461–1467, doi:10.1121/1.381892.
[22] W. Robert, J. Funnell, W.F. Decraemer, S.M. Khanna, On the damped frequency response of a finite-element model of the cat eardrum, J. Acoust. Soc. Am. 81 (1987) 1851–1859, doi:10.1121/1.394749.
[23] H. Wada, T. Metoki, T. Kobayashi, Analysis of dynamic behavior of human middle ear using a finite-element method, J. Acoust. Soc. Am. 92 (1992) 3157–3168, doi:10.1121/1.404211.
[24] T. Koike, H. Wada, T. Kobayashi, Modeling of the human middle ear using the finite-element method, J. Acoust. Soc. Am. 111 (2002) 1306–1317, doi:10.1121/1.1451073.
[25] R.Z. Gan, B. Feng, Q. Sun, Three-dimensional finite element modeling of human ear for sound transmission, Ann. Biomed. Eng. 32 (2004) 847–859, doi:10.1023/B:ABME.0000030260.22737.53.
[26] R.Z. Gan, T. Cheng, C. Dai, F. Yang, M.W. Wood, Finite element modeling of

sound transmission with perforations of tympanic membrane, J. Acoust. Soc. Am. 126 (2009) 243–253, doi:10.1121/1.3129129.
[27] J. Zhang, J. Tian, N. Ta, Z. Rao, Transient response of the human ear to impulsive stimuli: a finite element analysis, J. Acoust. Soc. Am. 143 (2018) 2768–2779, doi:10.1121/1.5026240.
[28] L. Caminos, J. Garcia-Manrique, A. Lima-Rodriguez, A. Gonzalez-Herrera, Analysis of the mechanical properties of the human tympanic membrane and its influence on the dynamic behaviour of the human hearing system, Appl. Bionics Biomech. 2018 (2018), doi:10.1155/2018/1736957.
[29] R.Z. Gan, Q. Sun, B. Feng, M.W. Wood, Acoustic-structural coupled finite element analysis for sound transmission in human ear-pressure distributions, Med. Eng. Phys. (2006), doi:10.1016/j.medengphy.2005.07.018.
[30] Y. Liu, S. Li, X. Sun, Numerical analysis of ossicular chain lesion of human ear, 25 (2009) 241–247. doi:10.1007/s10409-008-0206-6.
[31] A. Garcia-Gonzalez, C. Castro-Egler, A. Gonzalez-Herrera, Influence of the auditory system on pressure distribution in the ear canal, J. Mech. Med. Biol. 18 (2018), doi:10.1142/S0219519418500215.
[32] A. Garcia-Gonzalez, C. Castro-Egler, A. Gonzalez-Herrera, Analysis of the mechano-acoustic influence of the tympanic cavity in the auditory system, Biomed. Eng. Online 15 (2016), doi:10.1186/s12938-016-0149-2.
[33] X. Wang, T. Cheng, R.Z. Gan, Finite-element analysis of middle-ear pressure effects on static and dynamic behavior of human ear, J. Acoust. Soc. Am. 122 (2007) 906–917, doi:10.1121/1.2749417.
[34] T. Cheng, C. Dai, R.Z. Gan, Viscoelastic properties of human tympanic membrane, Ann. Biomed. Eng. 35 (2007) 305–314, doi:10.1007/s10439-006-9227-0.
[35] X. Zhang, R.Z. Gan, A comprehensive model of human ear for analysis of implantable hearing devices, IEEE Trans. Biomed. Eng. 58 (2011) 3024–3027, doi:10.1109/TBME.2011.2159714.
[36] A. Gonzalez-Herrera, E.S. Olson, A study of sound transmission in an abstract middle ear using physical and finite element models, J. Acoust. Soc. Am. 138 (2015) 2972–2985, doi:10.1121/1.4934515.
[37] A. Gonzalez-Herrera, J. Garcia-Manrique, Numerical study of the mechano-acoustic coupled resonance of a tube-membrane system, Meccanica 53 (2018) 3189–3207, doi:10.1007/s11012-018-0882-7.
[38] P. Razavi, H. Tang, J.J. Rosowski, C. Furlong, J.T. Cheng, Combined high-speed holographic shape and full-field displacement measurements of tympanic membrane, J. Biomed. Opt. (2018), doi:10.1117/1.jbo.24.3.031008.
[39] H. Tang, P. Razavi, K. Pooladvand, P. Psota, N. Maftoon, J.J.J. Rosowski, C. Furlong, J.T.J.T. Cheng, High-speed holographic shape and full-field displacement measurements of the tympanic membrane in normal and experimentally simulated pathological ears, Appl. Sci. 9 (2019), doi:10.3390/app9142809.
[40] P. Razavi, M.E. Ravicz, I. Dobrev, J.T. Cheng, C. Furlong, J.J. Rosowski, Response of the human tympanic membrane to transient acoustic and mechanical stimuli: preliminary results, Hear. Res. 340 (2016) 15–24, doi:10.1016/j.heares.2016.01.019.
[41] S. Seebacher, W. Osten, W.P.O. Jueptner, Measuring shape and deformation of small objects using digital holography, in: R.J. Pryputniewicz, G.M. Brown, W.P.O. Jueptner (Eds.), Laser Interferom. IX Appl., SPIE, 1998, p. 104, doi:10.1117/12.316439.
[42] C. Furlong, Absolute shape measurements using high-resolution optoelectronic holography methods, Opt. Eng. 39 (2000) 216, doi:10.1117/1.602355.
[43] I. Yamaguchi, T. Ida, M. Yokota, Surface shape measurement by phase-shifting digital holography with dual wavelengths, in: Interferom. XIII Tech. Anal., SPIE, 2006, p. 62920V, doi:10.1117/12.681970.
[44] J.J. Guinan, W.T. Peake, Middle-ear characteristics of anesthetized cats, J. Acoust. Soc. Am. 41 (1967), doi:10.1121/1.1910465.
[45] A. Gonzalez-Herrera, J. Tao Cheng, J.J. Rosowski, Analysis of the influence of the speaker position on the study of the dynamic behavior of a membrane combining holography technique and finite element models, 22nd Int. Congr. Sound Vib. ICSV 2015, 2015.
[46] G. Volandri, F. Di Puccio, P. Forte, C. Carmignani, Biomechanics of the tympanic membrane, J. Biomech. 44 (2011) 1219–1236, doi:10.1016/j.jbiomech.2010.12.023.
[47] X. Zhang, R.Z. Gan, Dynamic properties of human tympanic membrane – experimental measurement and modelling analysis, Int. J. Exp. Comput. Biomech. (2010), doi:10.1504/ijecb.2010.035260.
[48] J. Aernouts, J.R.M. Aerts, J.J.J. Dirckx, Mechanical properties of human tympanic membrane in the quasi-static regime from in situ point indentation measurements, Hear. Res. 290 (2012) 45–54, doi:10.1016/j.heares.2012.05.001.
[49] J. Fay, S. Puria, W.F. Decraemer, C. Steele, Three approaches for estimating the elastic modulus of the tympanic membrane, J. Biomech. (2005), doi:10.1016/j.jbiomech.2004.08.022.
[50] G. Volandri, F. Di Puccio, P. Forte, C. Carmignani, Biomechanics of the tympanic membrane, J. Biomech. (2011), doi:10.1016/j.jbiomech.2010.12.023.